THE JOURNAL OF PHYSICAL CHEMISTRY B

Article

pubs.acs.org/JPCB

Ultrafast Dynamics of C30 in Solution and within CDs and HSA Protein

Cristina Martin,[†] Boiko Cohen,[†] Issam Gaamoussi,[†,‡] Mustapha Ijjaali,[‡] and Abderrazzak Douhal*[,†]

[†]Departamento de Química Física, Facultad de Ciencias Ambientales y Bioquímica, and INAMOL, Universidad de Castilla-La Mancha, Avenida Carlos III, S/N, 45071 Toledo, Spain

[‡]Laboratorie de Chimie de la Matière Condensée, Faculté des Sciences et Techniques, University of Sidi Mohamed Ben Abdellah, Fez, Morocco 2202

Supporting Information

ABSTRACT: Steady-state UV−visible absorption and emission together with femto to nanosecond time-resolved emission techniques have been applied to study the dynamics of 3-(2-*N*-methylbenzimidazolyl)-7-(*N*,*N*-diethylamino)-coumarin (C30) in neat solvents, as well as in the presence of chemical (*β*-CD and DM-*β*-CD) and biological (HSA protein) cavities. The formation of inclusion complexes inside the hydrophobic CDs gives 1:1 and 1:2 guest:host complexes, whereas with the HSA protein, the formed 1:1 inclusion complexes are more robust. The picosecond experiments show the importance of the interactions of C30 with the medium, as well as the intramolecular events in the excited-state relaxation as evidenced by the increase in the global emission lifetime from ∼0.5 ns in MeOH/H_2O mixtures to 2.5 ns in THF, and to 1−3 ns when the dye is trapped within CDs and HSA cavities. Time-resolved anisotropy ($r(t)$) results indicate the involvement of ultrafast depolarization processes, whereas in the MeOH/H_2O mixtures $r(0)$ = 0.27, in DM-*β*-CD, $r(0)$ = 0.35. The rotational time decays clearly show the robustness of the formed complexes with CDs and HSA protein: ∼170 ps in MeOH/H_2O solvent mixtures, ∼850 ps due to 1:1 and 1:2 *β*-CD complexes, and 28 ns for HSA complexes. The femtosecond time-resolved emission experiments reveal the significant changes of the dynamics with the encapsulation of C30 by CDs (from approximately τ_1 = 0.3 and τ_2 = 2 ps in THF to approximately τ_1 = 1.0 and τ_2 = 7.5 ps in the MeOH/H2O binary mixture, and to approximately τ_1 = 3 and τ_2 = 30 ps in the CD complexes). The change is explained in terms of how the water molecules modulate the intramolecular charge transfer (ICT) time (τ_1) and how the restriction of the environment modifies the torsional process (τ_2). In the case of trapped C30 within the HSA protein the intermolecular interactions with the amino acid residues are revealed, giving rise to a complex photodynamical behavior due to the hydrophobic, H-bonding, electrostatic, and polar nature of the heterogeneous environment inside the protein. The protein confinement does not allow the occurrence of twisting motion in the trapped C30, and we observed a very fast (less than 100 fs) and slower (∼13 ps) ICT processes. We believe that the reported findings bring new knowledge for a better understanding of the photobehavior of coumarins in solution and trapped within hydrophobic pockets. The results can be applied to design better coumarin-based fluorescent labels for biological applications.

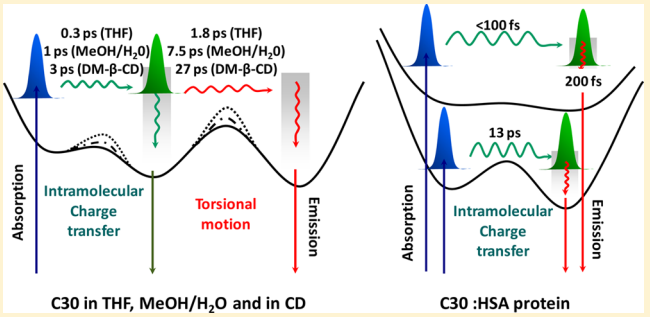

1. INTRODUCTION

Intimate information about the nature of the interactions between chromophores and chemical or biological cavities, as well as on the time scales of the involved processes, is crucial for the understanding of the overall activity of ligands and drugs in the human body, and for the development of effective fluorescent labels.[1−5] One can use advanced laser-based techniques to investigate the excited-state behavior and the structural transitions of dyes and drugs in solutions and in chemical and biological caging media, such as cyclodextrins and the human serum albumin (HSA) protein for example.[2,6−21]

HSA protein is the most abundant blood plasma protein. It plays an important role in the transport and distribution of various complex chemical and biological systems, such as drugs and steroid hormones.[22] The ligands bind to HSA in regions located in the hydrophobic cavities of subdomains IIA (binding site I) and IIIA (binding site II). Binding site I is dominated by strong hydrophobic interactions, whereas site II involves ion (dipole)−dipole, van der Waals, and/or H-bonding interactions. It has been demonstrated that the HSA protein undergoes reversible conformational transitions with changes in the pH that were also correlated with its solvation dynamics.[23]

Cyclodextrin (CD) nanocavities have drawn much attention in the last two decades due to their applications in several fields of science and technology such as drug delivery systems through the formation of inclusion complexes.[24−28] The

Received: March 17, 2014
Revised: April 25, 2014
Published: April 28, 2014

hydrophobic cavity of CDs generally leads to the alteration of the physical and chemical properties of the guest molecule.[29−33]

The coumarin dyes with benzopyrone structure constitute a class of compounds with many interesting properties, such as large molar extinction coefficient coupled with high quantum efficiency and strong solvent polarity-dependent Stokes shifts and are used in various applications in science and technology.[34−37] The representatives of the 7-aminocoumarin family have drawn much attention due to their broad use as fluorescent probes and their specific properties, such as sensitivity to changes in the local environment, for example.[37] They belong to a class of molecules characterized by an electron-donating group at the 7-position and electron acceptor group at the 3- or 4-position, which can exhibit a different charge transfer properties as a result of changes in the substituent or in the surrounding environment.[38] Several studies have assigned their nonradiative processes to a twisted intramolecular charge transfer (TICT)[39−43] or to open−close umbrella-like motion (ULM) of the amino group[44,45] that generally leads to nonfluorescent species. In this case the ultrafast intramolecular charge transfer (ICT) state quickly converts to TICT one by a twisting motion of the donor and acceptor moieties around the N−C bond linking the amino group to the rest of the chromophore.[46] In this type of reaction the hydrogen bonding with the environment plays a significant role and has to be taken into account.[44,45] Although several femtosecond studies on coumarins in solution have been reported,[34,47−49] there are only few on their interactions within nanocavities.[29,50−53] These have shown that the confinement by the cavities modifies the ultrafast solvation dynamics, affecting then the deactivation pathways of the formed entity. However, processes like ICT and twisting motion that can also take place in the formed complexes have not been fully characterized.

Here, we report on a femtosecond−nanosecond study of 3-(2-*N*-methylbenzimidazolyl)-7-*N*,*N*-diethylaminocoumarin (Scheme 1, Coumarin 30, C30) in tetrahydrofuran (THF), MeOH/H_2O binary mixture, and caged within *β*-cyclodextrin (*β*-CD), dimethyl-*β*-cyclodextrin (DM-*β*-CD), and HSA protein. The excited-state behavior of C30 is strongly dependent on the solvent polarity and hydrogen bonding ability.[43] It has been studied mostly in solution and its relaxation has been characterized predominantly on the picosecond time scale, whereas its ultrafast dynamics when trapped within chemical and biological hosts is not fully understood.[42,43] To study the effects that CD cavities exert on the stability and dynamics of the encapsulated C30, we have chosen as representatives the *β*-CD, a well-known and widely used in drug formulations natural cyclic oligosaccharide, and its dimethylated derivative (DM-*β*-CD). Finally, we have focused on the HSA protein as a representative of the blood plasma transport proteins to study the interactions of C30 with the amino acid residues of the protein binding sites, and the resulting effects on the structural and the dynamical properties of the guest and/or the host.[1] In the presence of the HSA protein C30 forms robust complexes with 1:1 stoichiometry, whereas in the presence of CDs we found 1:1 and 1:2 guest:host complexes. Time-resolved picosecond studies show that within the hydrophobic nanocavities the main decay channel has longer emission lifetime (from 460 ps to ∼2 ns). Time-resolved anisotropy measurements show different rotational times that depend on the nature cavity. When the molecule is inside the CDs, two rotational time constants were obtained corresponding to the free (∼180 ps) and complexed form (∼740 ps for *β*-CD and 990 ps for DM-*β*-CD). When C30 is interacting with HSA protein, a "dip−rise−dip" behavior in the anisotropy is found, explained in terms of two very different rotational times (180 ps and 28 ns). Femtosecond fluorescence up-conversion measurements show the slowing down of the initial dynamics of the caged C30 within the chemical and biological cavities, and the subsequent decrease of the charge transfer character due to the restriction of the twisting motion of the substituent.

Scheme 1. (A) Chemical Structure of 3-(2-*N*-Methylbenzimidazolyl)-7-(*N*,*N*-diethylamino)coumarin (C30) and the 1:1 (B) and 1:2 (C) Complexes of C30 in DM-*β*-CD and *β*-CD

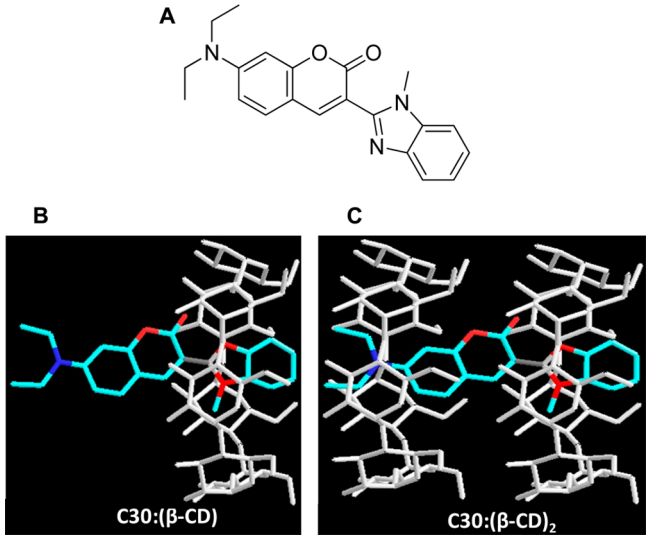

2. MATERIALS AND METHODS

Coumarin 30 (C30, 3-(2-*N*-methylbenzimidazolyl)-7-(*N*,*N*-diethylamino)coumarin, 99%, Sigma-Aldrich, Scheme 1), tetrahydrofuran (THF), methanol (MeOH, anhydrous, 99.8%, Sigma-Aldrich), *β*-CD and DM-*β*-CD (>99%, Cyclolab, Hungary), and the human serum albumin (HSA) protein (Fluka-Sigma-Aldrich, 99%) were used as received. In the case of C30:HSA, potassium phosphate buffer (0.1 M at pH 7) was used for the preparation of the samples. The measured values of pH in the MeOH/H_2O binary mixture were obtained using the AgCl electrode. The pH meter (Crison) was calibrated with standard solutions (pH 4 and pH 7, Crison) with an added 30% of MeOH, thus avoiding the effect of MeOH on the measured pH values. The measured pH of the pure 30% MeOH/H_2O mixture was 7, whereas that of the 30% MeOH/H_2O mixture in the presence of ∼9 mM *β*-CD was 6.5. The emission lifetimes were measured using a previously described time-correlated single-photon-counting picosecond spectrophotometer (Fluo-Time 200).[54] The sample was excited by a 40 ps pulsed (20 MHz) laser centered at 371 nm, and the emission signals were collected at the magic angle (54.7°). The instrument response function (IRF) was typically 65 ps. The emission decays were deconvoluted to the IRF and fitted to a multiexponential function using the Fluofit package (Picoquant).

The femtosecond emission transients have been collected using the fluorescence up-conversion technique. The system consists of a femtosecond Ti:sapphire oscillator MaiTai HP (Spectra Physics) and coupled to second harmonic generation

dx.doi.org/10.1021/jp5026575 | J. Phys. Chem. B 2014, 118, 5760−5771

and up-conversion setups.[18] The oscillator pulses (90 fs, 2.5 W, 80 MHz) were centered at 800 nm and doubled in an optical setup through a 0.5 mm BBO crystal to generate a pumping beam at 370 nm (~0.1 nJ). The polarization of the latter was set to magic angle with respect to the fundamental beam. The sample has been placed in a 1 mm thick rotating cell. The fluorescence was focused with reflective optics into a 0.3 mm BBO crystal and gated with the fundamental femtosecond beam. The IRF of the apparatus (measured as a Raman signal of pure solvent) was 200 fs (fwhm) for 370 nm excitation. To analyze the decays, a multiexponential function convoluted with the IRF was used to fit the experimental transients. All experiments were performed at 298 K.

The time-resolved picosecond anisotropy decay was constructed using the expression $r(t) = (I_{\parallel} - GI_{\perp})/(I_{\parallel} + 2GI_{\perp})$, where G is the ratio between the fluorescence intensity at parallel ($I_{\parallel}$) and perpendicular ($I_{\perp}$) polarizations of the emission with respect to the excitation beam. The value of G was measured at a gating window, in which the fluorescence is almost completely depolarized (tail-matching technique). The quality of the fits was characterized in terms of the residual distribution and reduced χ^2 values.

3. RESULTS AND DISCUSSION

3.1. Steady-State Studies. To begin with, we studied the steady-state behavior of Coumarin 30 (C30, Scheme 1) in a 30% MeOH/H_2O binary solution and in the presence of β-CD, DM-β-CD, and the HSA protein in water solutions (pH 7). Figure 1 shows the obtained UV−visible absorption (Figure 1A) and emission (Figure 1B) spectra. As a reference, the steady-state spectra of the dye in THF, a solvent with a polarity comparable to that of the CD interior, is also reported.

In a 30% MeOH/H_2O binary mixture (pH 7, Materials and Methods), the absorption spectrum of C30 (~5 × 10^{-6} M) is characterized by a single band corresponding to the S_0−S_1 transition with the maximum of absorption intensity positioned around 423 nm, which is in agreement with previously reported value for C30 in 30% EtOH/H_2O solution.[55] To confirm that only one prototropic form is present at S_0 in this mixture, we have measured the UV−visible absorption spectra (Figure 1S, Supporting Information) in the presence of HCl (pH = 3.9 and 6) and KOH (pH = 12). In the pH range 6−12, no changes in the absorption spectra were observed. Only at pH values below 4 was a significant red shift (from 422 to 446 nm) observed, due to the formation of the C30 cations. These results are in agreement with the reported pK_a values for a coumarin dye having a structure similar to that of C30 but having *N*-banzimidazolyl substituent at position 4 (pK_a^1 = 2.16 and pK_a^2 = 3.02 for the monocation).[56] Upon addition of 9 mM β-CD, the maximum absorption (416 nm) shifts by 7 nm (~400 cm^{-1}) to shorter wavelengths. The shift indicates formation of inclusion complexes between C30 and β-CD and is explained by a decrease in the C30 environment polarity within the CD cavity. We find a lower blue shift (~3 nm, ~170 cm^{-1}) in the absorption spectra of C30 upon addition of 7 mM DM-β-CD. Upon addition of 1.4 × 10^{-5} M HSA the absorption band intensity maximum (411 nm) shifts by 12 nm (~700 cm^{-1}), suggesting a stronger docking/encapsulation of the dye within the hydrophobic pockets of the protein, providing a less polar environment than the MeOH/H_2O binary mixture. A similar shift toward higher energies with a decrease of the environment polarity (solvent or hydrophobic pockets of the bovine serum albumin, BSA) has been reported for coumarin dyes.[43,57] The

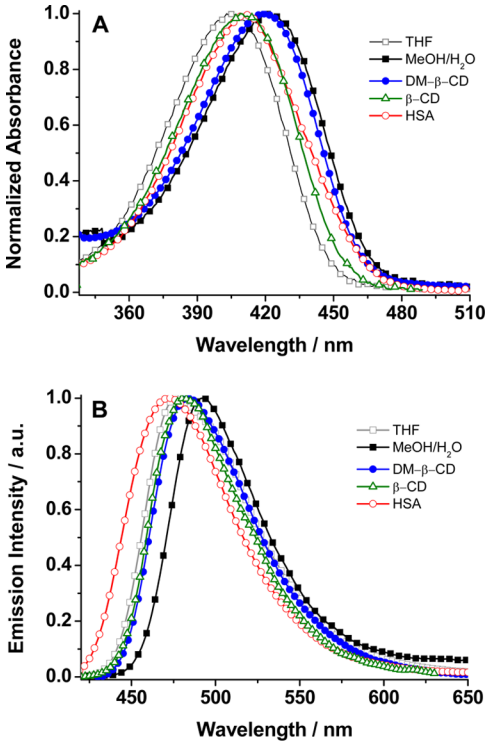

Figure 1. (A) UV−vis absorption spectra and (B) emission (λ_{exc} ~ 420 nm) spectra of 3-(2-*N*-Methylbenzimidazolyl)-7-*N*,*N*-diethylaminocoumarin (C30) in THF (open squares), 30% MeOH/H_2O binary solvent mixture (solid squares), the binary solvents mixture containing 9 mM β-CD (open triangles), the binary solvents mixture upon addition of 7.3 mM of DM-β-CD (solid circles), and aqueous buffer solution (pH ~ 7) containing 1.4 × 10^{-5} M human serum albumin (HSA) protein (open circles).

absorption spectrum of C30 in THF (an apolar solvent) is UV-shifted and its maximum of intensity is at 403 nm, which confirms that the local environment of C30 in the CD and HSA complexes is more apolar than in the MeOH/H_2O binary mixture.

Figure 1B shows the emission spectra of C30 in 30% MeOH/H_2O solutions, and in the presence of β-CD, DM-β-CD, and HSA protein following an excitation at 420 nm. The emission intensity maximum of C30 in 30% MeOH/H_2O binary solution (492 nm) is Stokes shifted by 69 nm (~3320 cm^{-1}), whereas that in THF is at 477 nm, showing the H-bonding and polarity effects on the emission spectrum position. In the presence of β-CD, DM-β-CD, and HSA protein, the spectra are also shifted to shorter wavelengths with respect to that using the binary mixture by 11 nm (465 cm^{-1}), 9 nm (380 cm^{-1}), and 20 nm (860 cm^{-1}), respectively. The blue shift is arising as a result of the encapsulation of the molecule by the hydrophobic and less polar hosts and the concomitant stabilization of the trapped C30. However, the change in the polarity of the local environment provided by the hosts in the complexes leads to a decrease in the values of the Stokes shift from 3320 cm^{-1} for the free C30 in the MeOH/H_2O binary mixture to 3250, 3106, and 3145 cm^{-1} in the presence of β-CD, DM-β-CD, and HSA protein, respectively. This decrease indicates a smaller electronic redistribution in the caged C30 or a weak destabilization of the excited species by ~100−200 cm^{-1} (depending on the host nature) when compared with the one in the MeOH/H_2O binary solution. The Stokes Shift

dx.doi.org/10.1021/jp5026575 | J. Phys. Chem. B 2014, 118, 5760−5771

obtained for C30 in THF solution (3850 cm^{-1}) differs significantly from the one obtained inside the cavities (3100–3300 cm^{-1}). This difference cannot be explained only by the environment polarity effect. For C30 one should consider the importance of the dihedral angle (θ) between the main coumarin part and the aromatic substituent, and the possibility for rotation around the single bond.[38,58,59] On the other hand, due to the encapsulation, the benzimidazole part can bend out of the main fluorophore plane and thus the rotation would be restricted. The observed decrease in the Stokes shift using the CDs and HSA cavities is a sign of restricted torsional motion between the two moieties of C30. Time-resolved experiments (see below) will give more information on the relevance of this restriction in the photodynamics of the caged C30.

To determine the binding constants (K_e) between C30 and the HSA protein, we have measured the change in the emission intensity of C30 at different concentrations and in the presence of 14 μM of HSA. The results were analyzed using eq 1S (Supporting Information), which assumes 1:1 stoichiometry of the formed complexes (Figure 2).[60] From the best fit we obtained $K_e = (2.2 \pm 0.1) \times 10^5$ M^{-1} at 298 K (n = 16, R^2 = 0.99297), which in turn gives $\Delta G^0 = -7.3 \pm 0.1$ kcal/mol. Comparable values of ΔG^0 and the binding constant have been reported for molecules with comparable chemical structures interacting with site 1 of domain II in the HSA protein.[61] The large value of the K_e indicates a robust C30–HSA complex.

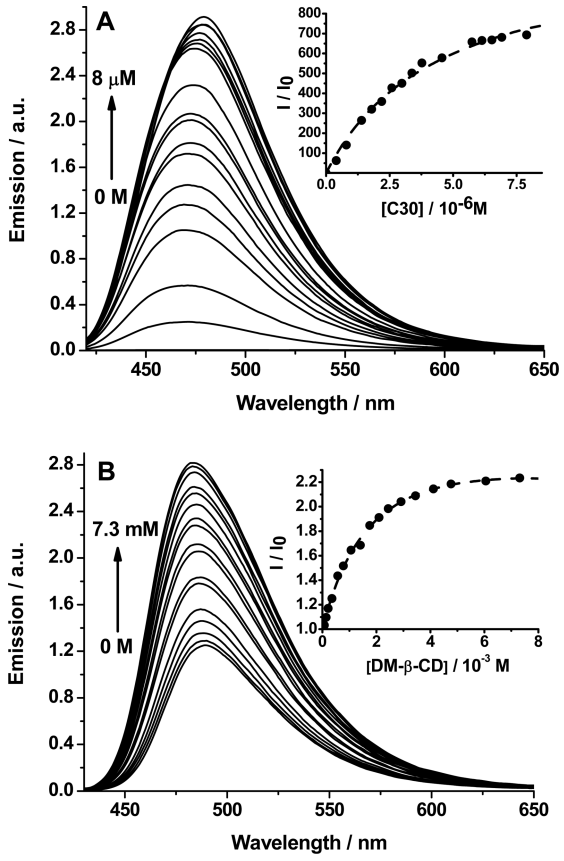

Figure 2. (A) Emission spectra of C30 at various concentrations and in the presence of 1.4×10^{-5} M HSA protein (pH ~ 7). The inset shows the change in the emission intensity (I/I_0) of the above solutions at 472 nm. The solid line shows the best fit assuming a 1:1 C30/HSA complex using a model described in the text. (B) Emission spectra of 5×10^{-6} M C30 in the presence of different concentrations of DM-β-CD in the 30% MeOH/H_2O binary solvent mixture. The inset shows the change in the emission intensity (I/I_0) at 483 nm at different DM-β-CD concentrations in the presence of C30 at 5×10^{-6} M. The solid line shows the best fit assuming 1:1 and 1:2 C30/DM-β-CD complexes using a model described in the text.

The emission spectra of C30 in the presence of different CD concentrations (Figure 2B and Figure 2S, Supporting Information) suggest formation of higher stoichiometry complexes. To obtain the binding constants of both 1:1 and 1:2 ($C30(CD)_2$) complexes (Figure 2), we applied eq 2S (Supporting Information).[62] We got $K_1 = 3220 \pm 50$ M^{-1} and $K_2 = 140 \pm 10$ M^{-1} (n = 10, R^2 = 0.99437), and $K_1 = 470 \pm 30$ M^{-1} and $K_2 = 63 \pm 10$ M^{-1} (n = 18, R^2 = 0.99726), for β-CD and DM-β-CD, respectively. Several studies on the interaction of coumarin dyes and CD derivatives have shown formation of 1:1 and 1:2 complexes.[29,37,63–66] Theoretical studies of C30:β-CD complexes have shown that the most stable 1:1 complex is the one having the encapsulation through the benzoimidazole part.[67] It should be noted that the value of K_1 for β-CD (3220 M^{-1}) is about an order of magnitude larger than the corresponding one for DM-β-CD (470 M^{-1}). This suggests that the presence of the methyl groups in the latter host disfavors the formation of more stable 1:1 complexes with comparison to the unmodified β-CD. One possible explanation is that the carbonyl group of the trapped C30 in β-CD is interacting with the OH one of this cavity forming more stable complexes.

3.2. Time-Resolved Studies. *3.2.1. Fluorescence Emission Lifetimes.* To get information on the photodynamics of free and trapped C30, we recorded the emission decays in THF, 30% MeOH/H_2O binary mixture and in the presence of β-CD, DM-β-CD, and HSA protein following an excitation at 371 nm, and gating at several representative wavelengths (465, 480, 500, 520, 540, and 560 nm). Figure 3 shows the decays

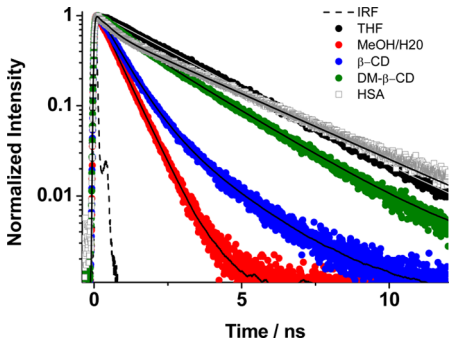

Figure 3. Time-correlated single-photon counting emission decays of C30 in the 30% MeOH/H_2O binary solvents mixture, in the binary solvents mixture containing β-CD and DM-β-CD, and in (HSA) protein buffer solution (pH ~ 7) observed at 480 nm, following an excitation at 371 nm. The dashed line is the IRF measured as scattered laser light.

collected at 480 nm, close to the maximum of the emission intensity (Figure 1B). The decays were fitted using multi-exponential functions (Table 1). For the THF solution the decay is monoexponential, giving a time constant of 2.50 ns. However, in 30% MeOH/H_2O solution the decay is biexponential, giving lifetimes (τ_i and pre-exponential factor a_i, %) of 460 ps (99%) and 1.65 ns (1%). The steady-state pH dependence studies in the MeOH/H_2O binary mixture solution confirm that C30 in this medium is present in a single (neutral)

dx.doi.org/10.1021/jp5026575 | J. Phys. Chem. B 2014, 118, 5760–5771

Table 1. Values of Time Constants (τ_i) and Normalized (to 100) Pre-exponential Factors (a_i) of the Multiexponential Functions Used in Fitting the Picosecond-Emission Transients of 3-(2-*N*-Methylbenzimidazolyl)-7-(*N*,*N*-diethylamino)coumarin (C30) in the Presence of Chemical (β-CD and DM-β-CD) and Biological (HSA Protein) Cavities at Different Wavelengths of Observation (λ_{obs}) after Picosecond Excitation at 371 nm

λ_{obs}/nm	τ_1/ns	a_1/%	τ_2/ns	a_2/%	τ_3/ns	a_3/%	χ^2
C30/β-CD in 30% MeOH/H_2O							
470	0.42	27	0.69	63	1.9	9	1.1
480		15		75		10	1.1
500		4		86		10	0.99
520				90		10	0.95
540				90		10	1.1
560				90		10	1.04
C30/DM-β-CD in 30% MeOH/H_2O							
470	0.40	23	1.36	26	2.31	51	0.99
480		20		26		54	1.10
500		18		26		56	1.05
520		16		26		58	1.09
540		15		26		59	1.07
560		13		26		61	1.01
C30/HSA in Buffer (pH = 7.1)							
470	0.37	24	2.94	77			1.2
480		26		74			1.1
500		33		67			1.02
520		41		60			1.03
540		42		58			1.02
560		42		58			1.02

prototropic form at S_0. The longer time component (1.65 ns) has a weak contribution and it is not very different from the value measured in MeOH (1.37 ns) and in EtOH (1.3 ns).[43] On the other hand, the picosecond time (460 ps) that has the major contribution was not reported in the single emission decay of C30 in 30% EtOH/H_2O (1.3 ns).[55] These differences reflect the high sensitivity of the C30 photodynamics to small variations in the solvent properties, such as H-bonding abilities and polarity.[43] The interactions of C30 with protic solvents (water, alcohols), having high polarity and strong H-bonding abilities, induces formation of stronger H-bonds, which increases the nonradiative decay rate constant as it has been observed for C30 in solution.[43] On the other hand, a two-state solvation model was proposed to describe the multiexponential behavior of the emission decays of coumarin 1 and coumarin 102 in several polar solvents.[68] Furthermore, a preferential solvation has been suggested to play a significant role in the photodynamics of excited coumarin chromophores in binary solvent mixtures.[69,70] Combining experimental and simulation data demonstrates that nanosized polar clusters are formed in binary solvents containing components with different dielectric properties as a medium response to charge redistribution upon photoexcitation of solute molecules.[63]

In the presence of β-CD (9×10^{-3} M), DM-β-CD (7.3×10^{-3} M), and HSA protein (1.4×10^{-5} M), the C30 aqueous solution decays are multiexponential (Figure 3) and reflect the heterogeneous nature of the systems (Table 1). For β-CD complexes, the global fit yields three components of 420 ps, 700 ps, and 1.9 ns, whereas in the presence of DM-β-CD these components are 400 ps, 1.36 ns, and 2.31 ns. The longest time constant (1.9 and 2.31 ns in the presence of β-CD and DM-β-CD, respectively) does not depend on the wavelength of observation (Table 1). This behavior is consistent with the presence of three populations of C30 in the presence of CDs, as is shown by the coexistence of 1:1 and 1:2 complexes in addition to the noncomplexed C30. The shortest time is assigned to this latter population (not encapsulated), and hence its value is not very far from the one obtained for C30 in 30% MeOH/H_2O solution (460 ps). The other two times are assigned to contributions from the 1:1 and 1:2 complexes. To assign these times to the specific complexes, we use the 2.5 ns one, observed in THF (a hydrophobic solvent). C30 trapped within two CD cavities will feel an environment not very different from the point of view of polarity and hydrophobicity to that of THF. Thus, we suggest that the 1.9 ns (2.31 ns) in the CDs solutions is due to 1:2 (C30:$(CD)_2$) complexes, whereas the 0.7 ns (1.36 ns) one is due to 1:1 entities. The hindrance of the twisting motion upon encapsulation of the C30 within the CD cavity, along with the increase in the hydrophobicity, results in the nonradiative deactivation pathway being less effective and hence the emissive intramolecular charge transfer (ICT) structure becomes the more stable one with fluorescence lifetime of 0.7 and 1.36 ns in β-CD and DM-β-CD, respectively. Formation of 1:2 complexes further impedes the H-bond formation and reduces the motion of the dye, resulting in longer emission lifetimes (1.9−2.3 ns).

The emission decays of C30 in the presence of HSA protein are biexponential and the global fit gives time constants of 370 ps and 2.94 ns. The shortest time is comparable to the one obtained for C30 in 30% MeOH/H_2O (460 ps) and for the free C30 in the presence of the CD cavities. Hence, we assign this component to a contribution of C30 in the buffer solution. The longest time component (2.91 ns) is arising from a population of C30 forming robust complexes with the HSA protein. This time is not very different from the observed value in THF (2.5 ns) and in other solvents with low polarity.[43] A theoretical and experimental docking study on several coumarin derivatives suggests that C30 interacts predominantly with site I of HSA domain IIA, dominated by strong hydrophobic interactions, while stabilizing its planar structure.[61] This additional stabilization of the emissive ICT structure results in a longer fluorescence lifetime as observed in the current study. For coumarin 35 interacting with BSA, the suppression of the TICT-state formation in the nonpolar and restrictive protein environment was suggested for the significant intensity enhancement and blue shift of the fluorescence band.[57] However, we believe that, in addition to the HSA confinement effect on the twisting motion of C30, the reduction in H-bonding interaction with water plays an important role in the decrease of the nonradiative process efficiency.[71−74]

3.2.2. Picosecond Time-Resolved Anisotropy. To get an insight on the rotational relaxation time of C30 in the complexes, we performed picosecond time-resolved emission anisotropy, ($r(t)$), measurements exciting at 371 nm and using 30% MeOH/H_2O binary mixture and aqueous solutions containing 9 mM β-CD, 7 mM DM-β-CD and 14 mM HSA protein (Figure 4).

For the 30% MeOH/H_2O binary mixture, $r(t)$ intensity decays fit to a single-exponential function giving a rotational time, $\phi = 171 \pm 30$ ps. This value is not very different from a previously published one for C30 in EtOH (121 ps).[75] Modeling C30 as a prolate ellipsoid, we calculated a rotational relaxation time of 111 and 48 ps, under stick- and slip-boundary condition limits, respectively.[76,77] This result indicates the

dx.doi.org/10.1021/jp5026575 | J. Phys. Chem. B 2014, 118, 5760−5771

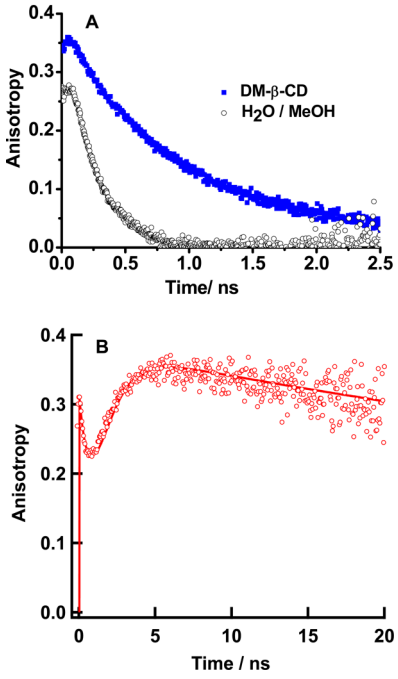

Figure 4. Decays of emission anisotropy, $r(t)$, of C30 (A) in the 30% MeOH/H_2O binary solvents mixture (open circles) upon addition of DM-β-CD (solid squares) and (B) in buffer solution (pH ~ 7) of HSA protein (full circles) collected at 480 nm and excited at 371 nm.

existence of significant friction between C30 and the surrounding MeOH/H_2O molecules slowing down its rotational relaxation time. The value of the initial anisotropy ($r(0)$ = 0.27) is lower than the ideal one (0.40), and it gives an angle of 23° between the transition moments of absorption and emission. This can be explained by the production of ICT state in the excited dye leading then to an electronic structure different from the absorbing one. In the presence of CDs, the anisotropy decays of C30 are biexponential, giving rotational time constants of ϕ_1 = 170 ± 30 ps (48%) and ϕ_2 = 740 ± 70 ps (52%) in the case of β-CD and ϕ_1 = 170 ± 30 ps (55%) and ϕ_2 = 990 ± 50 ps (45%) in the presence of DM-β-CD. The shortest time constant is fixed in the fit to take into account the population of nonencapsultaed C30. The second component (~0.7−1 ns) corresponds to the global contribution of the formed 1:1 and 1:2 complexes. In this case, we could not separate their contributions due to the two complexes having similar values of the rotational times, or as a result of a much weaker contribution from one of the component. The calculation of the molar fraction for the 1:1 and 1:2 β-CD complexes gives 0.97 and 0.01, respectively (see the Supporting Information for details of the calculation). Thus, ϕ_2 is mainly due to the 1:1 complex. On the other hand, in the presence of DM-β-CD the calculated molar fractions were 0.72 and 0.07 for the 1:1 and 1:2 complexes, respectively (see the Methods section of the Supporting Information). The initial value of the anisotropy decays in both CD cavities ($r(0)$ = 0.36) is closer to the ideal one and further indicates that the initial change in the transition moments is not as large as in free C30 ($r(0)$ = 0.27). The larger contribution of the component assigned to the encapsulated C30 in the presence of β-CD (a_2 = 52%) in comparison to the one in the presence of DM-β-CD (a_2 = 45%) can be explained with the higher affinity of β-CD to form complexes with C30, as evidenced by the larger value of its binding constant.

The time-resolved anisotropy decay of C30 interacting with the HSA protein has more complex behavior (Figure 4B). In addition to the decaying short and long anisotropy components, a rising component at intermediate times is also observed. This type of anisotropy decay is known as "dip−rise−dip" anisotropy profile, and it can be explained with the help of a two-component anisotropy model (eq 12S, Supporting Information), involving the presence of two species, each one characterized by its own lifetime and anisotropy decay.[78,79] The fit gives values for rotational time constants of ϕ_1 = 180 ps and ϕ_2 = 28 ns, with fluorescence lifetimes τ_1 = 370 ps and τ_2 = 2.9 ns. The values of ϕ_1 and τ_1 are not very different from the ones obtained for the free C30 in the 30% MeOH/H_2O binary mixtures (ϕ = 170 ps, τ = 460 ps), and hence we assign this contribution to a population of free C30 molecules in the buffer solution of HSA protein. The reported values for the global Brownian rotation of this protein are between 22 and 45 ns,[80,81] which is in agreement with the value of ϕ_2, and the fluorescence lifetime obtained from the fit corresponds to the lifetime of the C30:HSA protein complexes.[80,81] A similar value for the overall tumbling of the protein was reported for 7-dimethylamino-3-(4-maleimidophenyl)-4-methylcoumarin covalently bonded to HSA.[53] This result clearly indicates that the chromophore is strongly bound to the hydrophobic pocket of HSA and the robustness of the 1:1 complex between the dye and the protein is in agreement with the obtained large equilibrium constant (~2.2 × 10^5 M^{-1}). It has been shown that the "dip−rise−dip" anisotropy profile condition is better fulfilled for systems where internal motion is responsible for rapid nonradiative deactivation of the fluorescent state, such as coumarin 1, which is structurally similar to C30.[78] Such systems are characterized by a short fluorescence lifetime, whereas in the protein-bound condition, when the internal motion is severely restricted, a large increase in the lifetime occurs.

3.2.3. Femtosecond Fluorescence Study. To obtain detailed information on the early dynamics of C30 in THF, 30% MeOH/H_2O solution and in the presence of DM-β-CD and HSA protein, we measured the femtosecond emission transients at different wavelengths of observation upon excitation at 370 nm. Parts A and B of Figure 5 show the obtained transients for C30 in THF and MeOH/H_2O binary mixture solution, and sections A and B of Table 2 give the obtained time constants and pre-exponential factors using a multiexponential fit function convoluted with an IRF of 200 fs. The transients can be divided into two families: family I corresponding to the transients at wavelengths of observation around or lower than 460 nm, which we call blue transients, and family II, for observation at longer wavelengths (red transients). In the THF solution, the blue transients decay multiexponentially to a constant offset (nanosecond regime, resolved from the TCSPC measurements, 2.5 ns), with time constants of 0.3 and 1.8 ps. The contributions of both components decrease at 460 nm. At the red side of the spectrum (above 460 nm), the fit gives two rising components of 0.3 ps and ~1.8 ps. In the 30% MeOH/H_2O binary mixture, we observe a similar trend but the fast decaying (at 440−460 nm) and rising (at 480−580 nm) components have time constants of ~1 ps and ~7.5 ps. The offset is satisfactory fitted by ~0.5−1.2 ns.

In both cases, the values of the obtained short time constants rising at the red part of the spectra match the ones obtained as decay components at the blue side. The differences in the ultrafast components when comparing MeOH/H_2O solution to

dx.doi.org/10.1021/jp5026575 | J. Phys. Chem. B 2014, 118, 5760−5771

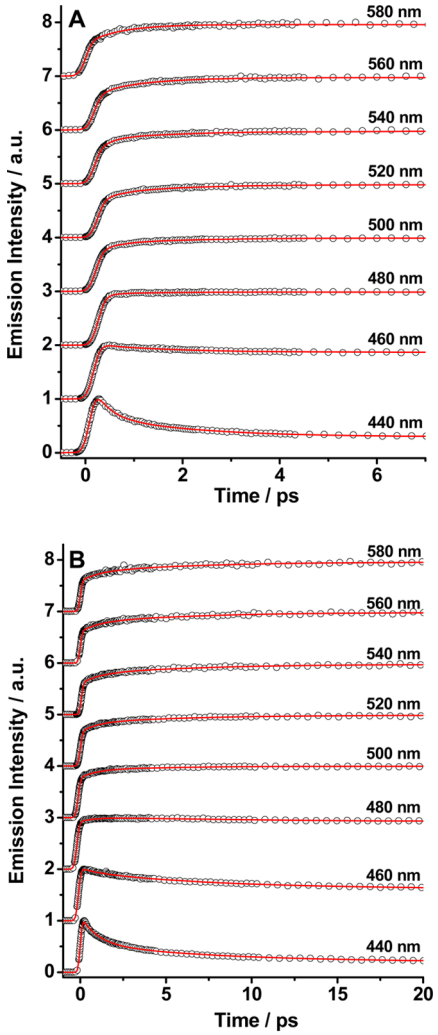

Figure 5. Femtosecond emission decays of C30 in (A) THF and in (B) the 30% MeOH/H_2O binary solvents mixture, gated at different emission wavelengths. The pump wavelength was 370 nm.

that of THF can be attributed to changes in the solvent polarity and the possibility of H-bonding interactions between the heteroatoms of C30 and the surrounding solvent molecules (Scheme 2). The very early solvation dynamics of various coumarin dyes in polar solvents are reported to take place within 50 fs.[82,83] Due to our time resolution (IRF ~ 200 fs) we cannot resolve correctly this ultrafast component in the emission decays. Hence, we consider the short time component of 0.3 ps in THF, ~1 ps in MeOH/H_2O solution a combination of several processes that include ultrafast solvation dynamics, intramolecular vibrational-energy redistribution (IVR) and the ICT process taking place in the excited C30. A clear change in the value of this time constant is observed when the nature of the solvent is altered. If we consider only the polarity of the solvent, the photoproduced ICT state should be more stabilized in the more polar MeOH/H_2O binary mixture (compared to the apolar THF) and the corresponding time-constant of its formation should be shorter.[84] However, we observe an opposite trend as the value of the time constant increases from 0.3 ps (THF) to ~1 ps in MeOH/H_2O mixture. This result is explained in terms of formation of H-bonds between C30 and the H-bonding solvent molecules, as it has been reported for other systems.[45] Two types of H-bonding

Table 2. Values of Time Constants (τ_i) and Normalized (to 100) Pre-exponential Factors (a_i) of the Multiexponential Functions Used in Fitting the Femtosecond-Emission Transients of 3-(2-*N*-Methylbenzimidazolyl)-7-(*N*,*N*-diethylamino)coumarin (C30) in THF (A) and in the 30% MeOH/H_2O Binary Solvent Mixture (B) at Different Wavelengths of Observation (λ_{obs}) after Femtosecond Excitation at 370 nm[a]

λ/nm	τ_1/ps (a_1/%)	τ_2/ps (a_2/%)	τ_3/ns (a_3/%)
	(A) THF		
440	0.29 (47)	1.8 (31)	0.78 (22)
460	0.24 (1)	1.8 (12)	1.03 (87)
480	(−) 0.22 (78)	(−) 1.8 (22)	1.08 (100)
500	(−) 0.27 (66)	(−) 1.8 (34)	1.28 (100)
520	(−) 0.30 (59)	(−) 1.8 (41)	1.30 (100)
540	(−) 0.31 (64)	(−) 1.9 (36)	1.14 (100)
560	(−) 0.32 (59)	(−) 1.7 (41)	1.28 (100)
580	(−) 0.29 (73)	(−) 1.9 (27)	1.12 (100)
	(B) 30% MeOH/H_2O Binary Solvent		
440	0.98 (49)	7.5 (32)	0.50 (19)
460	0.99 (7)	7.3 (31)	0.63 (62)
480	(−) 0.95 (100)	8.1 (7)	0.82 (93)
500	(−) 0.98 (67)	(−) 7.9 (33)	0.95 (100)
520	(−) 0.97 (51)	(−) 7.5 (49)	0.99 (100)
540	(−) 1.01 (45)	(−) 7.4 (55)	1.12 (100)
560	(−) 1.08 (45)	(−) 7.5 (55)	1.14 (100)
580	(−) 1.06 (44)	(−) 7.4 (56)	1.24 (100)

[a]Negative sign indicates rising component.

Scheme 2. Illustration of H-Bonding Interactions between C30 and Water (or Alcohol) Molecules and the Processes Taking Place in the Excited State (ICT: Intramolecular Charge Transfer, and Torsional Motion)

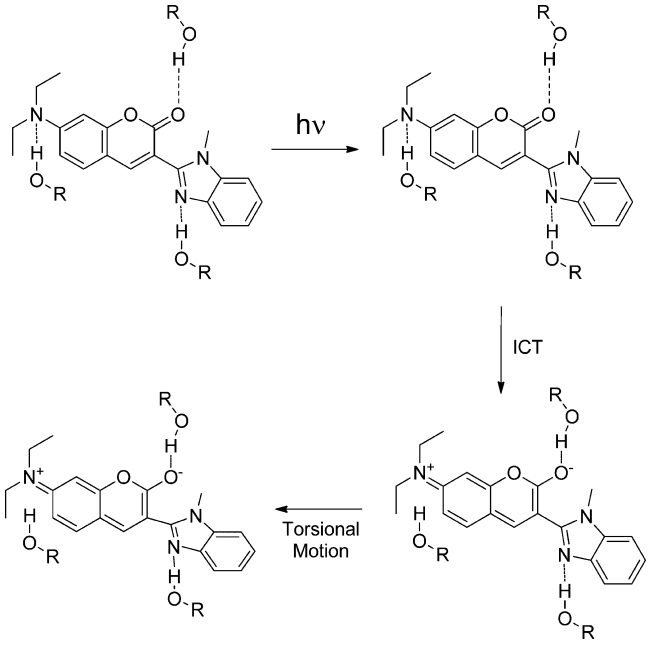

interactions have been suggested in the family of 7-amino-coumarines: (1) those involving the diethylamine and benzimidazole groups at the ground and excited states and (2) those involving interaction through the carbonyl electron acceptor group in the excited state.[44] For the occurrence of the ICT process in C30, where a charge is migrating from the

dx.doi.org/10.1021/jp5026575 | J. Phys. Chem. B 2014, 118, 5760−5771

Scheme 3. (Not to Scale) C30 Dynamics at S_1 in (A) THF (—) and Methanol/Water Mixtures (—·—), (B) DM-β-CD Solutions and (C) HSA Protein, Showing Two Dynamics Reflecting Different Specific and Nonspecific Interactions of C30 with the Local Environment (Amino Acids) of HSA

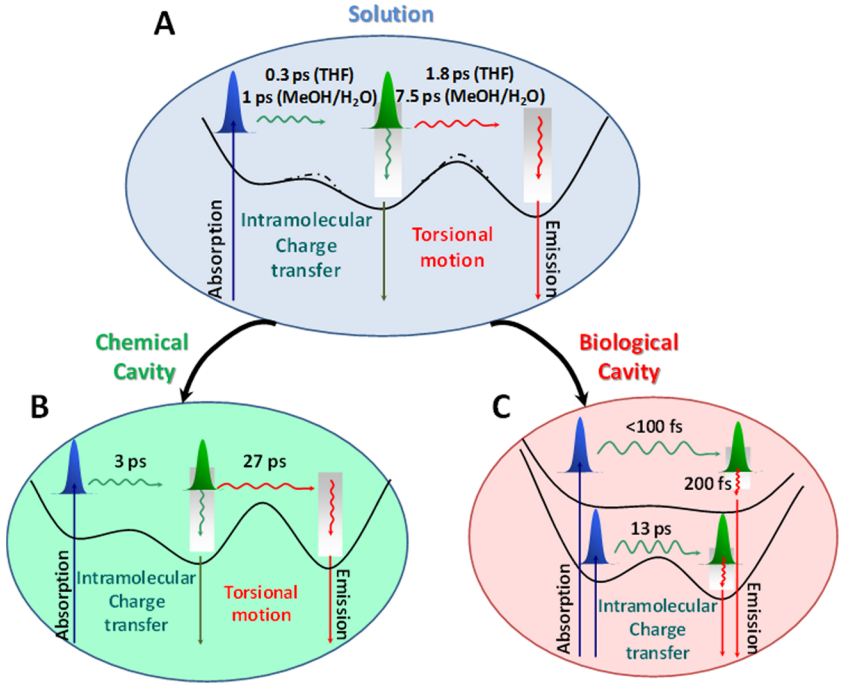

diethylamine group to the carbonyl one and benzimidazole receptor, the H-bonds with MeOH and/or water molecules should be weakened (or even broken) and strengthened (or formed), affecting the time constant of the intramolecular process. Scheme 2 illustrates a proposal for the involvement of H-bonds of C30 with MeOH and/or water molecules in the ICT process at the electronically excited state. Therefore, the ICT process in MeOH/H_2O binary mixtures has slower rate constants due to the formation and/or breaking of the intermolecular H-bonds. The picosecond time component (1.8−7.5 ps) is assigned to the torsional motion of the C−C single bond linking the two aromatic rings. Again, the specific H-bonding interactions with solvent molecules should be affecting the torsional time constant value. Here, in the MeOH/H_2O mixture, the time is longer (~7.5 ps) than in THF (~1.8 ps). Comparable behavior assigned to the H-bonding effect was observed for 4-nitropyrrolidinemethanol in which a bond swing around single bond occurs.[59] Scheme 3A illustrates the observed dynamics on potential energy curves at S_1, and which involves different energy barriers to ICT and the torsional motion to give the related species. To show that the observed changes in the ultrafast transients are not solely due to solvation dynamics, but involving formation of new species at S_1, we reconstructed the femtosecond time-resolved emission spectra (FRES) in THF and in MeOH/H_2O mixture, according to a procedure described elsewhere.[85] A clear isoemissive point is observed in both FRES (Figure 3S, Supporting Information). The existence of these isoemissive points indicates the contribution of additional deactivation pathways in the ultrafast relaxation dynamics of C30, which is in agreement with the suggested model.

The emission transients of C30 in the presence of 10^{-3} M of DM-β-CD clearly becomes slower but the trend is similar to the previous one (Figure 6A, Table 3A). In addition to the nanosecond offset, the multiexponential fit gives two short components having times of ~2.5 ps and ~26 ps decaying at the blue and rising at the red side, respectively. However, it should be noted that the biexponential fit only gives an approximate estimation of the slowing down of the initial photodynamics in the presence of CDs. This is due to the complex behavior of free and caged C30 dynamics, the heterogeneous nature of the CD solution, and the formed 1:1 and 1:2 complexes making difficult an accurate estimation of the time constants of their dynamics. Several studies on the solvation dynamics of coumarin dyes, such as coumarin 153 and 343 in the presence of γ-CD and di- and trimethylated β-CD, have demonstrated the multiexponential behavior of the solvation correlation function with at least three additional components arising from populations of encapsulated molecules forming several types of inclusion complexes.[66,83] The time scale of these processes spans from ~1 ps to several nanoseconds.[66,83] The slowing down of the initial dynamics of C30 in the presence of DM-β-CD (3 ps) observed here can be explained by the specific CD solvation of included guests.[29,50] DM-β-CD has seven OH groups (one for each pyranose unit) to interact with the water molecules found at the gate of the cavity.[29] The presence of this kind of biological-like water sets up slow solvation dynamics due to the restriction of the water molecules motion (diffusion and rotation) and the decrease in the cavity polarity.[29,50] The combination of these two effects shortens the formation time of the ICT state (Scheme 3B). Similar behavior has been observed not only for coumarin dyes but also for other molecules with ICT or excited-state intermolecular proton transfer properties as well.[4,21,25,30,86] Further restriction of the torsional motion of the benzimidazole substituent encapsulated within the CD cavities results in an increase in the longer time constant, as we actually observe (26 ps). It should be noted that for C30 interacting with CD cavities the reconstructed FRES is further complicated by the inherent heterogeneity of the systems.

dx.doi.org/10.1021/jp5026575 | J. Phys. Chem. B 2014, 118, 5760−5771

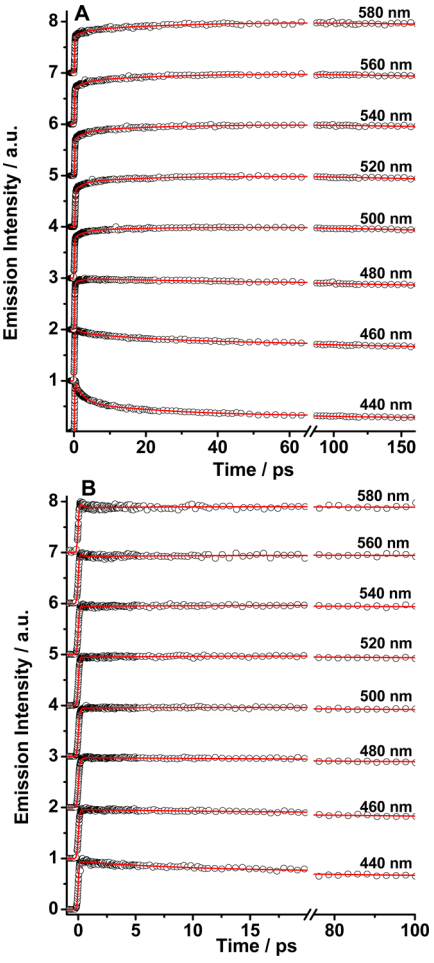

Figure 6. Femtosecond emission decays of C30 in the presence of (A) DM-β-CD and (B) HSA protein, gated at different emission wavelengths. The pump wavelength was 370 nm.

To get information on the ultrafast dynamics of the charge transfer and torsional motion of C30 into a biological cavity, we performed femtosecond-emission experiments on C30:HSA complexes, at different observation wavelengths. Figure 6B shows the fluorescence up-conversion transients of C30:HSA in pH 7 phosphate buffer, and Table 3B contains the obtained values of the time constants and pre-exponential factors of the fitting functions. Here the transients showing an offset of about 0.8−3 ns, can be divided into three families: (1) a transient at 440 nm, where the fast dynamics is described by a single 9.8 ps component; (2) transients in the 460−500 nm region, where we observe one rising component of 0.18 ps and a decaying one of ∼11−12 ps; and (3) transients for wavelengths of observation larger than 520 nm, which show a decay and a rise of ∼0.13 ps. The observation of the 0.18 ps decay component in the red region and rising in the blue one reveals the occurrence of a process not present in the CD complexes. The C30:HSA behavior can be explained by the heterogeneous nature of the interactions between the protein pockets and C30. Inside the protein the encapsulated dye will be subjected to specific and nonspecific interactions with the amino acid residues of the protein that will affect the rate of the involved reactions.[86,87] In addition, the local dielectric properties of the protein are inhomogeneous in nature and are strongly dependent on the local chemical environment, and hence, one should consider the protein relaxation microscopically.[88−90] The combination of H-bonds and electrostatic and hydrophobic interactions in the HSA environment will modify the dynamics of the trapped C30. It resides mainly within binding site I of subdomain IIA, as demonstrated by experimental and theoretical docking studies.[61] This study has identified two possible binding sites within subdomain IIA - site 1, with higher affinity toward C30, where several amino acid residues (arginine (Arg), lysine (Lys), and histidine (His)) can form H-bonds with the N and O atoms of the dye, and site 2 with lower affinity where the more hydrophobic amino acids such as valine (Val), leucine (Leu), and phenylalanine (Phe) can alter the local environment around the encapsulated C30, which in turn can affect the efficiency of the ICT.[61] Thus, we suggest two main different complexes of C30 with HSA that contribute to the emission transients (C1 and C2 of the same stoichiometry but C30 trapped in different ways). HSA:C30-1 should be closer to the amino acid residues (for example, Arg, Lys, and His), where H-bonds and electroctastic interactions are favorable, and as a result, the ICT has a solvation dynamics of ∼180 fs (Scheme 3C). The femtosecond component becomes a decay on the red side of the emission spectra. A similar effect has been reported for the tryptophan amino acid residue inside the HSA protein.[23] On the other hand, when the C30 is closer to the more hydrophobic amino acids (C2), the time constant of the ICT process is longer (∼13 ps), and we observe a decay and rise in the blue and red regions, respectively. Note that in both complexes, the rotation of the benzoimidazole substituent is not allowed due to the high confinement inside the HSA, as is clearly shown by the anisotropy results.

Scheme 3A,B,C shows a summary of the ultrafast photodynamics of the free C30 in THF, MeOH/H_2O binary mixture

Table 3. Values of Time Constants (τ_i) and Normalized (to 100) Pre-exponential Factors (a_i) of the Multiexponential Functions Used in Fitting the Femtosecond-Emission Transients of 3-(2-*N*-Methylbenzimidazolyl)-7-(*N*,*N*-diethylamino)coumarin (C30) in the 30% MeOH/H_2O Binary Solvent Mixture and in the Presence of Chemical DM-β-CD (A) and Biological HSA Protein (B) Cavities at Different Wavelengths of Observation (λ_{obs}) after Femtosecond Excitation at 370 nm[a]

λ/nm	τ_1/ps (a_1/%)	τ_2/ps (a_2/%)	τ_3/ns (a_3/%)
	(A) DM-β-CD Cavities		
440	2.41 (30)	25 (3)	1.10 (67)
460	2.55 (7)	27 (19)	1.42 (74)
480	(−) 2.40 (100)	26 (5)	1.73 (95)
500	(−) 2.61 (58)	(−) 26 (42)	1.72 (100)
520	(−) 2.44 (51)	(−) 28 (49)	1.54 (100)
540	(−) 2.75 (48)	(−) 29 (51)	2.49 (100)
560	(−) 2.65 (40)	(−) 28 (60)	1.80 (100)
580	(−) 2.56 (33)	(−) 27 (67)	2.49 (100)
	(B) Biological HSA Protein Cavities		
440		9.8 (19)	0.75 (81)
460	(−) 0.17 (100)	11.9 (5)	1.00 (95)
480	(−) 0.18 (100)	11.7 (2)	1.56 (98)
500	(−) 0.17 (79)	(−) 11.2 (21)	1.75 (100)
520		(−) 12.6 (100)	1.97 (100)
540	0.18 (3)	(−) 13.6 (100)	2.58 (97)
560	0.17 (15)	(−) 13 (100)	2.60 (85)
580	0.17 (23)	(−) 13 (100)	3.00 (77)

[a]Negative sign indicates rising component.

dx.doi.org/10.1021/jp5026575 | J. Phys. Chem. B 2014, 118, 5760−5771

and interacting with chemical and biological cavities in the excited states. The difference in the observed time is due H-bonding, polarity, and the confinement effect, in this case, CD and HSA protein cavities. For C30:HSA, we observed two different trajectories/dynamics reflecting specific and non-specific interactions in the confinement, reflecting the effect on the related dynamics.

4. CONCLUSION

The steady-state results show that upon interaction with the CD cavities, C30 forms inclusion complexes of 1:1 and 1:2 guest:host stoichiometry, whereas with the HSA protein the complexes are only 1:1 type. The TCSPC measurements demonstrate that in binary MeOH/H_2O mixture the non-emissive channel operates effectively, whereas in the inclusion complexes this mechanism is inaccessible due to the reduced polarity and lower H-bonding ability of the local environment. The time-resolved anisotropy indicates strong interactions with the solvent in the binary mixture giving a rotational time of ∼170 ps. For 1:1 and 1:2 β-CD complexes the global rotational time is around 900 ps. For the 1:1 C30:HSA robust complexes the rotational time is ∼28 ns. The femtosecond experiments reveal the slowing down of the stepwise dynamics upon encapsulation of C30 (from ∼1 and 7 ps in the binary solvent mixture to ∼3 and 26 ps in the CD complexes) and it is explained in terms of a slow solvation dynamics of the water molecules around the gates of the CD cavities and cavity confinement. Upon interaction with the HSA the molecular structure of C30 allows interacting with the charged amino acid residues, as well as to reside within a more apolar environment in the vicinity of the more hydrophobic amino acids. The strong docking of C30 does not permit a twisting motion, whereas very fast (less than 100 fs) and slow (∼13 ps) ICT processes were observed.

We believe that the reported findings and the related discussion bring new knowledge for a better understanding of the molecular behavior of this dye. Furthermore, the results might be relevant to the design of specific fluorescent molecular probes for biological systems.

■ ASSOCIATED CONTENT

Supporting Information

Additional information about the binding constant, molar fraction, and dip rise dip anisotropy calculations, absorption spectra of C30 in MeOH/water (30/70) mixtures at several pHs, emission spectra of C30 at various concentrations of β-CD, and the reconstructed FRES for THF and the MeOH/H_2O mixture upon excitation at 370 nm. This material is available free of charge via the Internet at http://pubs.acs.org.

■ AUTHOR INFORMATION

Corresponding Author

*A. Douhal: e-mail, Abderrazzak.Douhal@uclm.es; phone, +34-925-265717.

Notes

The authors declare no competing financial interest.

■ ACKNOWLEDGMENTS

This work was supported by the MICINN through projects MAT2011-25472, UNCM08-1E-068, UNCM08-1E-050. CM thanks MEC for the FPU fellowship. We thank Prof. Pilar Lillo from Instituto de Química Física "Rocasolano" CSIC, Madrid, for her help with the analysis of the anisotropy of the C30:HSA protein complexes.

■ REFERENCES

(1) Zhong, D. P.; Douhal, A.; Zewail, A. H. Femtosecond Studies of Protein-Ligand Hydrophobic Binding and Dynamics: Human Serum Albumin. *Proc. Natl. Acad. Sci. U. S. A.* **2000**, *97*, 14056−14061.

(2) Zhong, D. P.; Pal, S. K.; Wan, C. Z.; Zewail, A. H. Femtosecond Dynamics of a Drug-Protein Complex: Daunomycin with Apo Riboflavin-Binding Protein. *Proc. Natl. Acad. Sci. U. S. A.* **2001**, *98*, 11873−11878.

(3) Mataga, N.; Chosrowjan, H.; Taniguchi, S. Investigations into the Dynamics and Mechanisms of Ultrafast Photoinduced Reactions Taking Place in Photoresponsive Protein Nanospaces (PINS). *J. Photochem. Photobiol., C* **2004**, *5*, 155−168.

(4) Douhal, A.; Sanz, M.; Tormo, L. Femtochemistry of Orange II in Solution and in Chemical and Biological Nanocavities. *Proc. Natl. Acad. Sci. U. S. A.* **2005**, *102*, 18807−18812.

(5) Narayanan, S. S.; Pal, S. K. Nonspecific Protein-DNA Interactions: Complexation of Alpha-Chymotrypsin with a Genomic DNA. *Langmuir* **2007**, *23*, 6712−6718.

(6) Cuny, G. D.; Landgrebe, K. D.; Smith, T. P.; Fehr, M. J.; Petrich, J. W.; Carpenter, S. Photoactivated Virucidal Properties of Tridentate 2−2′-Dihydroxy Azobenzene and 2-Salicylideneaminophenol Platinum Pyridine Complexes. *Bioorg. Med. Chem. Lett.* **1999**, *9*, 237−240.

(7) Das, K.; Smirnov, A. V.; Wen, J.; Miskovsky, P.; Petrich, J. W. Photophysics of Hypericin and Hypocrellin a in Complex with Subcellular Components: Interactions with Human Serum Albumin. *Photochem. Photobiol.* **1999**, *69*, 633−645.

(8) Wen, J.; Chowdhury, P.; Wills, N. J.; Wannemuehler, Y.; Park, J.; Kesavan, S.; Carpenter, S.; Kraus, G. A.; Petrich, J. W. Toward the Molecular Flashlight: Preparation, Properties, and Photophysics of a Hypericin-Luciferin Tethered Molecule. *Photochem. Photobiol.* **2002**, *76*, 153−157.

(9) El-Kemary, M.; Gil, M.; Douhal, A. Relaxation Dynamics of Piroxicam Structures within Human Serum Albumin Protein. *J. Med. Chem.* **2007**, *50*, 2896−2902.

(10) Tormo, L.; Organero, J. A.; Cohen, B.; Martin, C.; Santos, L.; Douhal, A. Dynamical and Structural Changes of an Anesthetic Analogue in Chemical and Biological Nanocavities. *J. Phys. Chem. B* **2008**, *112*, 13641−13647.

(11) Lu, Z.; Zhang, Y.; Liu, H.; Yuan, J.; Zheng, Z.; Zou, G. Transport of a Cancer Chemopreventive Polyphenol, Resveratrol: Interaction with Serum Albumin and Hemoglobin. *J. Fluoresc.* **2007**, *17*, 580−587.

(12) Monti, S.; Manet, I.; Manoli, F.; Sortino, S. Binding and Photochemistry of Enantiomeric 2-(3-Benzoylphenyl)Propionic Acid (Ketoprofen) in the Human Serum Albumin Environment. *Photochem. Photobiol. Sci.* **2007**, *6*, 462−470.

(13) Vaya, I.; Jimenez, M. C.; Miranda, M. A. Excited-State Interactions in Flurbiprofen-Tryptophan Dyads. *J. Phys. Chem. B* **2007**, *111*, 9363−9371.

(14) Zhang, L.; Kao, Y.-T.; Qiu, W.; Wang, L.; Zhong, D. Femtosecond Studies of Tryptophan Fluorescence Dynamics in Proteins: Local Solvation and Electronic Quenching. *J. Phys. Chem. B* **2006**, *110*, 18097−18103.

(15) Chergui, M.; Zewail, A. H. Electron and X-Ray Methods of Ultrafast Structural Dynamics: Advances and Applications. *ChemPhysChem* **2009**, *10*, 28−43.

(16) Lin, M. M.; Shorokhov, D.; Zewail, A. H. Conformations and Coherences in Structure Determination by Ultrafast Electron Diffraction. *J. Phys. Chem. A* **2009**, *113*, 4075−4093.

(17) Yurtsever, A.; Zewail, A. H. 4d Nanoscale Diffraction Observed by Convergent-Beam Ultrafast Electron Microscopy. *Science* **2009**, *326*, 708−712.

(18) Gil, M.; Douhal, A. Femtosecond Dynamics in Ionic Structures of a Heart Medicine. *Chem. Phys. Lett.* **2006**, *432*, 106−109.

(19) Gil, M.; Douhal, A. Femtosecond Dynamics of a Non-Steroidal Anti-Inflammatory Drug (Piroxicam) in Solution: The Involvement of Twisting Motion. *Chem. Phys.* **2008**, *350*, 179−185.
(20) Gil, M.; Douhal, A. Femtosecond Dynamics of Piroxicam Structures in Solutions. *J. Phys. Chem. A* **2008**, *112*, 8231−8237.
(21) Cohen, B.; Organero, J. A.; Santos, L.; Padial, L. R.; Douhal, A. Exploring the Ground and Excited States Structural Diversity of Levosimendan, a Cardiovascular Calcium Sensitizer. *J. Phys. Chem. B* **2010**, *114*, 14787−14795.
(22) Peters, J. T. *All About Albumin: Biochemistry, Genetics, and Medical Applications*; Academic Press: San Diego, 1995; p 432.
(23) Qiu, W.; Zhang, L.; Okobiah, O.; Yang, Y.; Wang, L.; Zhong, D.; Zewail, A. H. Ultrafast Solvation Dynamics of Human Serum Albumin: Correlations with Conformational Transitions and Site-Selected Recognition. *J. Phys. Chem. B* **2006**, *110*, 10540−10549.
(24) Cal, K.; Centkowska, K. Use of Cyclodextrins in Topical Formulations: Practical Aspects. *Eur. J. Pharm. Biopharm.* **2008**, *68*, 467−478.
(25) El-Kemary, M.; Organero, J. A.; Santos, L.; Douhal, A. Effect of Cyclodextrin Nanocavity Confinement on the Photorelaxation of the Cardiotonic Drug Milrinone. *J. Phys. Chem. B* **2006**, *110*, 14128−14134.
(26) Marconi, G.; Monti, S.; Manoli, F.; Degli Esposti, A.; Mayer, B. A Circular Dichroism and Structural Study of the Inclusion Complex Artemisinin-B-Cyclodextrin. *Chem. Phys. Lett.* **2004**, *383*, 566−571.
(27) Zhang, J.; Ma, P. X. Host-Guest Interactions Mediated Nano-Assemblies Using Cyclodextrin- Containing Hydrophilic Polymers and Their Biomedical Applications. *Nano Today* **2010**, *5*, 337−350.
(28) Chen, Y.; Liu, Y. Cyclodextrin-Based Bioactive Supramolecular Assemblies. *Chem. Soc. Rev.* **2010**, *39*, 495−505.
(29) Douhal, A. Ultrafast Guest Dynamics in Cyclodextrin Nanocavities. *Chem. Rev.* **2004**, *104*, 1955−1976.
(30) Martín, C.; Gil, M.; Cohen, B.; Douhal, A. Ultrafast Photodynamics of Drugs in Nanocavities: Cyclodextrins and Human Serum Albumin Protein. *Langmuir* **2012**, *28*, 6746−6759.
(31) Szente, L.; Szemán, J. Cyclodextrins in Analytical Chemistry: Host−Guest Type Molecular Recognition. *Anal. Chem.* **2013**, *85*, 8024−8030.
(32) Anand, R.; Manoli, F.; Manet, I.; Daoud-Mahammed, S.; Agostoni, V.; Gref, R.; Monti, S. B-Cyclodextrin Polymer Nanoparticles as Carriers for Doxorubicin and Artemisinin: A Spectroscopic and Photophysical Study. *Photochem. Photobiol. Sci.* **2012**, *11*, 1285−1292.
(33) Anand, R.; Ottani, S.; Manoli, F.; Manet, I.; Monti, S. A Close-up on Doxorubicin Binding to γ-Cyclodextrin: An Elucidating Spectroscopic, Photophysical and Conformational Study. *RSC Adv.* **2012**, *2*, 2346−2357.
(34) Horng, M. L.; Gardecki, J. A.; Papazyan, A.; Maroncelli, M. Subpicosecond Measurements of Polar Solvation Dynamics: Coumarin 153 Revisited. *J. Phys. Chem.* **1995**, *99*, 17311−17337.
(35) Jin, H.; Baker, G. A.; Arzhantsev, S.; Dong, J.; Maroncelli, M. Solvation and Rotational Dynamics of Coumarin 153 in Ionic Liquids: Comparisons to Conventional Solvents. *J. Phys. Chem. B* **2007**, *111*, 7291−7302.
(36) Maroncelli, M.; Zhang, X.-X.; Liang, M.; Roy, D.; Ernsting, N. P. Measurements of the Complete Solvation Response of Coumarin 153 in Ionic Liquids and the Accuracy of Simple Dielectric Continuum Predictions. *Faraday Discuss.* **2012**, *154*, 409−424.
(37) Wagner, B. D. The Use of Coumarins as Environmentally-Sensitive Fluorescent Probes of Heterogeneous Inclusion Systems. *Molecules* **2009**, *14*, 210−237.
(38) Liu, X.; Xu, Z.; Cole, J. M. Molecular Design of Uv−Vis Absorption and Emission Properties in Organic Fluorophores: Toward Larger Bathochromic Shifts, Enhanced Molar Extinction Coefficients, and Greater Stokes Shifts. *J. Phys. Chem. C* **2013**, *117*, 16584−16595.
(39) Jones, G.; Jackson, W. R.; Choi, C. Y.; Bergmark, W. R. Solvent Effects on Emission Yield and Lifetime for Coumarin Laser Dyes. Requirements for a Rotatory Decay Mechanism. *J. Phys. Chem.* **1985**, *89*, 294−300.
(40) Rechthaler, K.; Köhler, G. Excited State Properties and Deactivation Pathways of 7-Aminocoumarins. *Chem. Phys.* **1994**, *189*, 99−116.
(41) Rettig, W.; Klock, A. Intramolecular Fluorescence Quenching in Aminocoumarines. Identification of an Excited State with Full Charge Separation. *Can. J. Chem.* **1985**, *63*, 1649−1653.
(42) Satpati, A. K.; Kumbhakar, M.; Nath, S.; Pal, H. Photophysical Properties of Coumarin-7 Dye: Role of Twisted Intramolecular Charge Transfer State in High Polarity Protic Solvents. *Photochem. Photobiol.* **2009**, *85*, 119−129.
(43) Senthilkumar, S.; Nath, S.; Pal, H. Photophysical Properties of Coumarin-30 Dye in Aprotic and Protic Solvents of Varying Polarities. *Photochem. Photobiol.* **2004**, *80*, 104−111.
(44) Lopez Arbeloa, T.; Lopez Arbeloa, F.; Tapia, M. J.; Lopez Arbeloa, I. Hydrogen-Bonding Effect on the Photophysical Properties of 7-Aminocoumarin Derivatives. *J. Phys. Chem.* **1993**, *97*, 4704−4707.
(45) Chipem, F. A. S.; Mishra, A.; Krishnamoorthy, G. The Role of Hydrogen Bonding in Excited State Intramolecular Charge Transfer. *Phys. Chem. Chem. Phys.* **2012**, *14*, 8775−8790.
(46) Bhattacharyya, K.; Chowdhury, M. Environmental and Magnetic Field Effects on Exciplex and Twisted Charge Transfer Emission. *Chem. Rev.* **1993**, *93*, 507−535.
(47) Adhikari, A.; Sahu, K.; Dey, S.; Ghosh, S.; Mandal, U.; Bhattacharyya, K. Femtosecond Solvation Dynamics in a Neat Ionic Liquid and Ionic Liquid Microemulsion: Excitation Wavelength Dependence. *J. Phys. Chem. B* **2007**, *111*, 12809−12816.
(48) Kovalenko, S. A.; Ruthmann, J.; Ernsting, N. P. Ultrafast Strokes Shift and Excited-State Transient Absorption of Coumarin 153 in Solution. *Chem. Phys. Lett.* **1997**, *271*, 40−50.
(49) Glasbeek, M.; Zhang, H. Femtosecond Studies of Solvation and Intramolecular Configurational Dynamics of Fluorophores in Liquid Solution. *Chem. Rev.* **2004**, *104*, 1929−1954.
(50) Bhattacharyya, K. Nature of Biological Water: A Femtosecond Study. *Chem. Commun.* **2008**, 2848−2857.
(51) Sarkar, N.; Datta, A.; Das, S.; Bhattacharyya, K. Solvation Dynamics of Coumarin 480 in Micelles. *J. Phys. Chem.* **1996**, *100*, 15483−15486.
(52) Sen, P.; Roy, D.; Mondal, S. K.; Sahu, K.; Ghosh, S.; Bhattacharyya, K. Fluorescence Anisotropy Decay and Solvation Dynamics in a Nanocavity: Coumarin 153 in Methyl B-Cyclodextrins. *J. Phys. Chem. A* **2005**, *109*, 9716−9722.
(53) Mandal, U.; Ghosh, S.; Mitra, G.; Adhikari, A.; Dey, S.; Bhattacharyya, K. A Femtosecond Study of the Interaction of Human Serum Albumin with a Surfactant (SDS). *Chem.—Asian J.* **2008**, *3*, 1430−1434.
(54) Organero, J. A.; Tormo, L.; Douhal, A. Caging Ultrafast Proton Transfer and Twisting Motion of 1-Hydroxy-2-Acetonaphthone. *Chem. Phys. Lett.* **2002**, *363*, 409−414.
(55) Jones, G., II; Jimenez, J. A. C. Azole-Linked Coumarin Dyes as Fluorescence Probes of Domain-Forming Polymers. *J. Photochem. Photobiol., B* **2001**, *65*, 5−12.
(56) Kirpichënok, M. A.; Patalakha, N. S.; Fomina, L. Y.; Grandberg, I. I. Spectral-Luminescence Properties and Acid-Base Properties of Luminophores Obtained from 3-Iodo-7-Dialkylaminocoumarins. *Chem. Heterocycl. Compd.* **1991**, *27*, 934−939.
(57) Nag, A.; Bhattacharyya, K. Role of Twisted Intramolecular Charge Transfer in the Fluorescence Sensitivity of Biological Probes: Diethylaminocoumarin Laser Dyes. *Chem. Phys. Lett.* **1990**, *169*, 12−16.
(58) Rafiq, S.; Rajbongshi, B. K.; Nair, N. N.; Sen, P.; Ramanathan, G. Excited State Relaxation Dynamics of Model Green Fluorescent Protein Chromophore Analogs: Evidence for Cis−Trans Isomerism. *J. Phys. Chem. A* **2011**, *115*, 13733−13742.
(59) Rafiq, S.; Yadav, R.; Sen, P. Femtosecond Excited-State Dynamics of 4-Nitrophenyl Pyrrolidinemethanol: Evidence of Twisted Intramolecular Charge Transfer and Intersystem Crossing Involving the Nitro Group. *J. Phys. Chem. A* **2011**, *115*, 8335−8343.

(60) Organero, J. A.; Douhal, A. Confinement Effects on the Photorelaxation of a Proton-Transfer Phototautomer. *Chem. Phys. Lett.* **2003**, *373*, 426−431.
(61) Shobini, J.; Mishra, A. K.; Sandhya, K.; Chandra, N. Interaction of Coumarin Derivatives with Human Serum Albumin: Investigation by Fluorescence Spectroscopic Technique and Modeling Studies. *Spectrochim. Acta, Part A* **2001**, *57*, 1133−1147.
(62) Tormo, L.; Organero, J. A.; Douhal, A. Effect of Nanocavity Confinement on the Relaxation of Anesthetic Analogues: Relevance to Encapsulated Drug Photochemistry. *J. Phys. Chem. B* **2005**, *109*, 17848−17854.
(63) Bergmark, W. R.; Davis, A.; York, C.; Macintosh, A.; Jones, G. Dramatic Fluorescence Effects for Coumarin Laser Dyes Coincluded with Organic Solvents in Cyclodextrins. *J. Phys. Chem.* **1990**, *94*, 5020−5022.
(64) Scypinski, S.; Drake, J. M. Photophysics of Coumarin Inclusion Complexes with Cyclodextrin. Evidence for Normal and Inverted Complex Formation. *J. Phys. Chem.* **1985**, *89*, 2432−2435.
(65) Al-Kindy, S. M. Z.; Suliman, F. E. O.; Al-Hamadi, A. A. Fluorescence Enhancement of Coumarin-6-Sulfonyl Chloride Amino Acid Derivatives in Cyclodextrin Media. *Anal. Sci.* **2001**, *17*, 539−543.
(66) Sen, P.; Roy, D.; Mondal, S. K.; Sahu, K.; Ghosh, S.; Bhattacharyya, K. Fluorescence Anisotropy Decay and Solvation Dynamics in a Nanocavity: Coumarin 153 in Methyl Beta-Cyclodextrins. *J. Phys. Chem. A* **2005**, *109*, 9716−9722.
(67) Holubekova, A.; Mach, P.; Urban, J. Spectral Properties of Coumarin Derivatives in Various Environments. *Cent. Eur. J. Chem.* **2013**, *11*, 492−501.
(68) Yip, R. W.; Wen, Y. X.; Szabo, A. G. Decay Associated Fluorescence Spectra of Coumarin 1 and Coumarin 102: Evidence for a Two-State Solvation Kinetics in Organic Solvents. *J. Phys. Chem.* **1993**, *97*, 10458−10462.
(69) Agmon, N. The Dynamics of Preferential Solvation. *J. Phys. Chem. A* **2002**, *106*, 7256−7260.
(70) Petrov, N. A Fluorescence Spectroscopy Study of Preferential Solvation in Binary Solvents. *High Energy Chem.* **2006**, *40*, 22−34.
(71) Fayed, T. A.; Organero, J. A.; Garcia-Ochoa, I.; Tormo, L.; Douhal, A. Ultrafast Twisting Motions and Intramolecular Charge-Transfer Reaction in a Cyanine Dye Trapped in Molecular Nanocavities. *Chem. Phys. Lett.* **2002**, *364*, 108−114.
(72) Nag, A.; Kundu, T.; Bhattacharyya, K. Effect of Solvent Polarity on the Yield of Twisted Intramolecular Charge Transfer (TICT) Emission. Competition between Formation and Nonradiative Decay of the TICT State. *Chem. Phys. Lett.* **1989**, *160*, 257−260.
(73) Van Gompel, J. A.; Schuster, G. B. Photophysical Behavior of Ester-Substituted Aminocoumarins: A New Twist. *J. Phys. Chem.* **1989**, *93*, 1292−1295.
(74) Avouris, P.; Gelbart, W. M.; El-Sayed, M. A. Nonradiative Electronic Relaxation under Collision-Free Conditions. *Chem. Rev.* **1977**, *77*, 793−833.
(75) Jerebtsov, S.; Kolomenskii, A.; Poudel, M.; Zhu, F.; Schuessler, H. Lifetime and Anisotropy Decay of Excited Coumarin 30 Measured by a Femtosecond Pump−Probe Technique. *J. Mod. Opt.* **2006**, *53*, 2609−2617.
(76) Hu, C. M.; Zwanzig, R. Rotational Friction Coefficients for Spheroids with Slipping Boundary-Condition. *J. Chem. Phys.* **1974**, *60*, 4354−4357.
(77) Baskin, J. S.; Zewail, A. H. Molecular Structure and Orientation: Concepts from Femtosecond Dynamics. *J. Phys. Chem. A* **2001**, *105*, 3680−3692.
(78) Bhattacharya, B.; Nakka, S.; Guruprasad, L.; Samanta, A. Interaction of Bovine Serum Albumin with Dipolar Molecules: Fluorescence and Molecular Docking Studies. *J. Phys. Chem. B* **2009**, *113*, 2143−2150.
(79) Ludescher, R. D.; Peting, L.; Hudson, S.; Hudson, B. Time-Resolved Fluorescence Anisotropy for Systems with Lifetime and Dynamic Heterogeneity. *Biophys. Chem.* **1987**, *28*, 59−75.
(80) Castellano, F. N.; Dattelbaum, J. D.; Lakowicz, J. R. Long-Lifetime Ru(II) Complexes as Labeling Reagents for Sulfhydryl Groups. *Anal. Biochem.* **1998**, *255*, 165−170.
(81) Ferrer, M. L.; Duchowicz, R.; Carrasco, B.; de la Torre, J. G.; Acuna, A. U. The Conformation of Serum Albumin in Solution: A Combined Phosphorescence Depolarization-Hydrodynamic Modeling Study. *Biophys. J. .* **2001**, *80*, 2422−2430.
(82) Jimenez, R.; Fleming, G. R.; Kumar, P. V.; Maroncelli, M. Femtosecond Solvation Dynamics of Water. *Nature* **1994**, *369*, 471−473.
(83) Vajda, S.; Jimenez, R.; Rosenthal, S. J.; Fidler, V.; Fleming, G. R.; Castner, E. W., Jr. Femtosecond to Nanosecond Solvation Dynamics in Pure Water and inside the γ-Cyclodextrin Cavity. *J. Chem. Soc., Faraday Trans.* **1995**, *91*, 867−873.
(84) Grabowski, Z. R.; Rotkiewicz, K.; Rettig, W. Structural Changes Accompanying Intramolecular Electron Transfer: Focus on Twisted Intramolecular Charge-Transfer States and Structures. *Chem. Rev.* **2003**, *103*, 3899−4032.
(85) Qin, Y.; Chang, C.-W.; Wang, L.; Zhong, D. Validation of Response Function Construction and Probing Heterogeneous Protein Hydration by Intrinsic Tryptophan. *J. Phys. Chem. B* **2012**, *116*, 13320−13330.
(86) Cohen, B.; Alvarez, C. M.; Carmona, N. A.; Organero, J. A.; Douhal, A. Proton-Transfer Reaction Dynamics within the Human Serum Albumin Protein. *J. Phys. Chem. B* **2011**, *115*, 7637−7647.
(87) Friedman, R. Proton Transfer on the Molecular Surface of Proteins and Model Systems. *Isr. J. Chem.* **2009**, *49*, 149−153.
(88) Patargias, G. N.; Harris, S. A.; Harding, J. H. A Demonstration of the Inhomogeneity of the Local Dielectric Response of Proteins by Molecular Dynamics Simulations. *J. Chem. Phys.* **2010**, *132*, 235103.
(89) Schutz, C. N.; Warshel, A. What Are the Dielectric "Constants" of Proteins and How to Validate Electrostatic Models? *Prot. Struct. Funct. Bioinf.* **2001**, *44*, 400−417.
(90) Sham, Y. Y.; Muegge, I.; Warshel, A. The Effect of Protein Relaxation on Charge-Charge Interactions and Dielectric Constants of Proteins. *Biophys. J. .* **1998**, *74*, 1744−1753.